Inorg. Chem. **2006**, *45*, 11019–11029

Extended Dipolar Nonlinear Optical Chromophores Based on *trans*-Bis[1,2-phenylenebis(dimethylarsine)]chlororuthenium(II) Centers

Benjamin J. Coe,*,† Josephine L. Harries,† James A. Harris,‡ Bruce S. Brunschwig,‡ Peter N. Horton,§ and Michael B. Hursthouse§

School of Chemistry, University of Manchester, Oxford Road, Manchester M13 9PL, U.K., Molecular Materials Research Center, Beckman Institute, MC 139-74, California Institute of Technology, 1200 East California Blvd., Pasadena, California 91125, and EPSRC National Crystallography Service, School of Chemistry, University of Southampton, Highfield, Southampton SO17 1BJ, U.K.

Received September 1, 2006

Four new complex salts *trans*-$[Ru^{II}Cl(pdma)_2L_A][PF_6]_n$ [pdma = 1,2-phenylenebis(dimethylarsine); L_A = 1,4-bis[*E*-2-(4-pyridyl)ethenyl]benzene (bpvb), $n = 1$, **1**; L_A = *N*-methyl-1,4-bis(*E*-2-(4-pyridyl)ethenyl)benzene ($Mebpvb^+$), $n = 2$, **2**; L_A = *N*-phenyl-1,4-bis(*E*-2-(4-pyridyl)ethenyl)benzene ($Phbpvb^+$), $n = 2$, **3**; L_A = *N*-(2-pyrimidyl)-1,4-bis-(*E*-2-(4-pyridyl)ethenyl)benzene ($Pymbpvb^+$), $n = 2$, **4**] have been prepared. The electronic absorption spectra of **1**–**4** display intense, visible metal-to-ligand charge-transfer (MLCT) bands, with λ_{max} values in the range 432–474 nm in acetonitrile. Intense intraligand charge-transfer (ILCT) bands due to L_A are also observed, with λ_{max} values in the range 350–416 nm. Cyclic voltammetric studies in acetonitrile reveal reversible $Ru^{III/II}$ waves with $E_{1/2}$ values of ca. 1.05 V vs Ag/AgCl, together with L_A-based reduction processes that are irreversible with the exception of **1**. Salts **1**–**4** have been investigated by using Stark (electroabsorption) spectroscopy in butyronitrile glasses at 77 K. These studies have afforded dipole moment changes, $\Delta\mu_{12}$, for the MLCT and ILCT transitions which have been used to calculate molecular static first hyperpolarizabilities, β_0, according to the two-state equation $\beta_0 = 3\Delta\mu_{12}(\mu_{12})^2/(E_{max})^2$ (μ_{12} = transition dipole moment, E_{max} = MLCT/ILCT energy). In contrast with related Ru^{II} ammine complexes, replacement of a central *E*-ethylene bond with a 1,4-phenylene unit does not appear to be an especially effective strategy for combating the NLO transparency-efficiency tradeoff in these pdma complexes. Single-crystal X-ray studies with the complex salts **2** and **3** and also with the pro-ligand salt $[Phbpvb^+]PF_6 \cdot 0.5HPF_6$ show that these materials all adopt centrosymmetric packing structures.

Introduction

Organic nonlinear optical (NLO) materials hold promise for applications in various emerging optoelectronic and photonic technologies.[1] Fundamental research with such materials has involved a diverse range of organotransition metal complexes which can combine very marked NLO effects with various other potentially useful properties such as redox and/or magnetic behavior.[2] Previous studies in our laboratory have involved the use of hyper-Rayleigh scattering (HRS)[3] and electronic Stark effect (electroabsorption)[4] spectroscopic measurements to assess the quadratic NLO responses of various metal complexes of pyridinium-substituted ligands, mostly based on Ru^{II} centers.[2n,5] We have found that such chromophores can exhibit very large static first hyperpolarizabilities, β_0, that are associated with intense, low-energy metal-to-ligand charge-transfer (MLCT) transitions. The quantity β_0 represents the intrinsic NLO response in the absence of any resonance and is especially relevant to practical applications where absorption must be avoided. Perhaps more significantly, we have also demonstrated

* To whom correspondence should be addressed. E-mail: b.coe@manchester.ac.uk.
† University of Manchester.
‡ California Institute of Technology.
§ University of Southampton.

(1) (a) *Nonlinear Optical Properties of Organic Molecules and Crystals*; Chemla, D. S., Zyss, J., Eds.; Academic Press: Orlando, FL, 1987; Vols. 1 and 2. (b) *Molecular Nonlinear Optics: Materials, Physics and Devices*; Zyss, J.; Academic Press: Boston, 1994. (c) *Organic Nonlinear Optical Materials* (*Advances in Nonlinear Optics, Vol. 1.*); Bosshard, Ch., Sutter, K., Prêtre, Ph., Hulliger, J., Flörsheimer, M., Kaatz, P., Günter, P.; Gordon and Breach: Amsterdam, 1995. (d) *Nonlinear Optics of Organic Molecules and Polymers*; Nalwa, H. S., Miyata, S., Eds.; CRC Press: Boca Raton, FL, 1997. (e) Marder, S. R. *Chem. Commun.* **2006**, 131. (f) *Nonlinear Optical Properties of Matter: From Molecules to Condensed Phases*; Papadopoulos, M. G.; Leszczynski, J.; Sadlej, A. J., Eds.; Springer: Dordrecht, 2006.

10.1021/ic061659u CCC: $33.50
Published on Web 12/06/2006

reversible switching of NLO responses by using redox changes in Ru^{II} complexes[6] and via protonation of cyanide ligands in Fe^{II} complexes.[7]

Extending the length of a π-conjugated system is a common approach to increasing the β_0 responses of dipolar organic molecules.[1] In donor−acceptor (D−A) polyenes, the addition of *E*-ethenyl units generally decreases the intramolecular charge-transfer (ICT) energy, E_{max}, and increases the accompanying dipole moment change, $\Delta\mu_{12}$. In accord with the widely applied two-state model,[8] these changes lead to large increases in NLO responses and D−A polyenes have been found to possess some of the largest β_0 values known.[9] The fact that increases in NLO activity are generally accompanied by increased visible absorption is often referred to as the "transparency-efficiency tradeoff". In contrast with polyenyl systems, D−A oligo(phenylenevinylene) chromophores, in which the conjugated bridge contains alternating 1,4-phenylene rings and *E*-CH═CH units, show increases of ICT E_{max} values on extension of conjugation.[10] The incorporation of *E*,*E*-1,4-bis(ethenyl)phenylene bridges into purely organic dipolar chromophores has therefore been proposed as a strategy for increasing optical transparency and stability while maintaining relatively large NLO responses.[11] In previous studies with Ru^{II} ammine complexes of the ligand *N*-methyl-1,4-bis-(*E*-2-(4-pyridyl)ethenyl)-benzene ($Mebpvb^+$), we have achieved large β_0 values combined with increased optical transparencies, when compared with related polyenyl chromophores.[5a] The present work involves the synthesis of new *N*-aryl analogues of $Mebpvb^+$ and their complexation, together with that of $Mebpvb^+$, to the *trans*-$\{Ru^{II}Cl(pdma)_2\}^+$ [pdma = 1,2-phenylenebis(dimethylarsine)] electron-donor center.

Experimental Section

Materials and Procedures. The pro-ligand pdma was obtained from Dr G. Reid, University of Southampton. The compounds *trans*-$[Ru^{II}Cl(pdma)_2(NO)][PF_6]_2$,[12] 2-[2-(4-formylphenyl)ethenyl]pyridine (FEP),[13] *N*-phenyl-4-picolinium chloride ($[Phpic^+]Cl$),[14] *N*-(2-pyrimidyl)-4-picolinium hexafluorophosphate ($[Pympic^+]PF_6$),[14] and 1,4-bis[*E*-2-(4-pyridyl)ethenyl]benzene (bpvb)[15] were synthesized according to published procedures. All other reagents were obtained commercially and used as supplied. All reactions were performed under an argon atmosphere. Products were dried in a vacuum desiccator ($CaSO_4$) for ca. 24 h prior to characterization.

General Physical Measurements. ^1H NMR spectra were recorded on a Varian XL-300 or a Bruker 500 spectrometer, and all shifts are referenced to TMS. The fine splitting of pyridyl or phenyl ring AA′BB′ patterns is ignored and the signals are reported as simple doublets, with *J* values referring to the two most intense peaks. Elemental analyses were performed by the Microanalytical Laboratory, University of Manchester, and UV−vis spectra were obtained by using a Hewlett-Packard 8452A diode array spectrophotometer. Mass spectra were recorded using +electrospray on a Micromass Platform spectrometer.

Cyclic voltammetric measurements were carried out with an EG&G PAR model 283 potentiostat/galvanostat. An EG&G PAR K0264 single-compartment microcell was used with a silver/silver chloride reference electrode separated by a salt bridge from a Pt disk working electrode and Pt wire auxiliary electrode. Acetonitrile (HPLC grade) was distilled before use, and $[NBu^n_4]PF_6$, twice recrystallized from ethanol and dried in vacuo, was used as supporting electrolyte. Solutions containing ca. 10^{-3} M analyte (0.1 M electrolyte) were deaerated by purging with N_2. All $E_{1/2}$ values were calculated from $(E_{pa} + E_{pc})/2$ at a scan rate of 200 mV s^{-1}.

Synthesis of *N*-Phenyl-1,4-bis(*E*-2-(4-pyridyl)ethenyl)benzene Chloride, [Phbpvb$^+$]Cl. $[Phpic^+]Cl\cdot 1.25H_2O$ (100 mg, 0.438 mmol) and FEP (108 mg, 0.516 mmol) were dissolved in methanol (1 mL) and heated to reflux. Pyridine (1 drop) was added, and the mixture was heated under reflux for a further 3.5 h. The dark brown

(2) (a) Kanis, D. R.; Ratner, M. A.; Marks, T. J. *Chem. Rev.* **1994**, *94*, 195. (b) Long, N. J. *Angew. Chem., Int. Ed. Engl.* **1995**, *34*, 21. (c) Whittall, I. R.; McDonagh, A. M.; Humphrey, M. G.; Samoc, M. *Adv. Organomet. Chem.* **1998**, *42*, 291. (d) Whittall, I. R.; McDonagh, A. M.; Humphrey, M. G.; Samoc, M. *Adv. Organomet. Chem.* **1998**, *43*, 349. (e) Heck, J.; Dabek, S.; Meyer-Friedrichsen, T.; Wong, H. *Coord. Chem. Rev.* **1999**, *1217*, 190−192. (f) Gray, G. M.; Lawson, C. M. In *Optoelectronic Properties of Inorganic Compounds*; Roundhill, D. M.; Fackler, J. P., Jr., Eds.; Plenum: New York, 1999; pp 1−27. (g) Shi, S. In *Optoelectronic Properties of Inorganic Compounds*; Roundhill, D. M.; Fackler, J. P., Jr., Eds.; Plenum: New York, 1999; pp 55−105. (h) Le Bozec, H.; Renouard, T. *Eur. J. Inorg. Chem.* **2000**, 229. (i) Barlow, S.; Marder, S. R. *Chem. Commun.* **2000**, 1555. (j) Lacroix, P. G. *Eur. J. Inorg. Chem.* **2001**, 339. (k) Di Bella, S. *Chem. Soc. Rev.* **2001**, *30*, 355. (l) Coe, B. J. In *Comprehensive Coordination Chemistry II*; McCleverty, J. A., Meyer, T. J., Eds.; Elsevier Pergamon: Oxford, U.K., 2004; Vol. 9, pp 621−687. (m) Cariati, E.; Pizzotti, M.; Roberto, D.; Tessore, F.; Ugo, R. *Coord. Chem. Rev.* **2006**, *250*, 1210. (n) Coe, B. J. *Acc. Chem. Res.* **2006**, *39*, 383.

(3) (a) Clays, K.; Persoons, A. *Phys. Rev. Lett.* **1991**, *66*, 2980. (b) Hendrickx, E.; Clays, K.; Persoons, A. *Acc. Chem. Res.* **1998**, *31*, 675.

(4) (a) Liptay, W. In *Excited States*; Lim, E. C., Ed.; Academic Press: New York, 1974; Vol. 1, pp 129−229. (b) Bublitz, G. U.; Boxer, S. G. *Annu. Rev. Phys. Chem.* **1997**, *48*, 213.

(5) Selected recent examples: (a) Coe, B. J.; Jones, L. A.; Harris, J. A.; Brunschwig, B. S.; Asselberghs, I.; Clays, K.; Persoons, A.; Garín, J.; Orduna, J. *J. Am. Chem. Soc.* **2004**, *126*, 3880. (b) Coe, B. J.; Harris, J. A.; Jones, L. A.; Brunschwig, B. S.; Song, K.; Clays, K.; Garín, J.; Orduna, J.; Coles, S. J.; Hursthouse, M. B. *J. Am. Chem. Soc.* **2005**, *127*, 4845. (c) Coe, B. J.; Harris, J. A.; Brunschwig, B. S.; Asselberghs, I.; Clays, K.; Garín, J.; Orduna, J. *J. Am. Chem. Soc.* **2005**, *127*, 13399. (d) Coe, B. J.; Harries, J. L.; Helliwell, M.; Brunschwig, B. S.; Harris, J. A.; Asselberghs, I.; Hung, S.-T.; Clays, K.; Horton, P. N.; Hursthouse, M. B. *Inorg. Chem.* **2006**, *45*, 1215.

(6) (a) Coe, B. J.; Houbrechts, S.; Asselberghs, I.; Persoons, A. *Angew. Chem., Int. Ed.* **1999**, *38*, 366. (b) Coe, B. J. *Chem.−Eur. J.* **1999**, *5*, 2464.

(7) Coe, B. J.; Harries, J. L.; Helliwell, M.; Jones, L. A.; Asselberghs, I.; Clays, K.; Brunschwig, B. S.; Harris, J. A.; Garín, J.; Orduna, J. *J. Am. Chem. Soc.* **2006**, *128*, 12192.

(8) (a) Oudar, J. L.; Chemla, D. S. *J. Chem. Phys.* **1977**, *66*, 2664. (b) Oudar, J. L. *J. Chem. Phys.* **1977**, *67*, 446.

(9) Selected examples: (a) Marder, S. R.; Cheng, L.-T.; Tiemann, B. G.; Friedli, A. C.; Blanchard-Desce, M.; Perry, J. W.; Skindhøj, J. *Science* **1994**, *263*, 511. (b) Blanchard-Desce, M.; Alain, V.; Bedworth, P. V.; Marder, S. R.; Fort, A.; Runser, C.; Barzoukas, M.; Lebus, S.; Wortmann, R. *Chem.−Eur. J.* **1997**, *3*, 1091. (c) Lawrentz, U.; Grahn, W.; Lukaszuk, K.; Klein, C.; Wortmann, R.; Feldner, A.; Scherer, D. *Chem.−Eur. J.* **2002**, *8*, 1573.

(10) Selected examples: (a) Meier, H.; Petermann, R.; Gerold, J. *Chem. Commun.* **1999**, 977. (b) Meier, H.; Gerold, J.; Kolshorn, H.; Baumann, W.; Bletz, M. *Angew. Chem., Int. Ed.* **2002**, *41*, 292. (c) Meier, H.; Gerold, J.; Jacob, D. *Tetrahedron Lett.* **2003**, *44*, 1915.

(11) Selected examples: (a) Alain, V.; Rédoglia, S.; Blanchard-Desce, M.; Lebus, S.; Lukaszuk, K.; Wortmann, R.; Gubler, U.; Bosshard, C.; Günter, P. *Chem. Phys.* **1999**, *245*, 51. (b) Luo, J.-D.; Hua, J.-L.; Qin, J.-G.; Cheng, J.-Q.; Shen, Y.-C.; Lu, Z.-H.; Wang, P.; Ye, C. *Chem. Commun.* **2001**, 171.

(12) Douglas, P. G.; Feltham, R. D.; Metzger, H. G. *J. Am. Chem. Soc.* **1971**, *93*, 84.

(13) Ichimura, K.; Watanabe, S. *J. Polym. Sci. Polymer Chem. Ed.* **1982**, *20*, 1419.

(14) Coe, B. J.; Harris, J. A.; Asselberghs, I.; Clays, K.; Olbrechts, G.; Persoons, A.; Hupp, J. T.; Johnson, R. C.; Coles, S. J.; Hursthouse, M. B.; Nakatani, K. *Adv. Funct. Mater.* **2002**, *12*, 110.

(15) Amoroso, A. J.; Cargill Thompson, A. M. W.; Maher, J. P.; McCleverty, J. A.; Ward, M. D. *Inorg. Chem.* **1995**, *34*, 4828.

solution was cooled to room temperature and diethyl ether was added to afford a brown precipitate, which was collected by filtration and washed with diethyl ether. Purification was effected by precipitation from methanol/diethyl ether to afford a yellow solid. Yield: 95 mg (48%). δ_H(300 MHz, CD_3OD) 9.04 (2 H, d, $J = 6.7$ Hz, C_5H_4N), 8.34 (2 H, d, $J = 6.7$ Hz, C_5H_4N), 8.11 (1 H, d, $J = 15.5$ Hz, CH), 7.86−7.58 (15 H, C_5H_4N + 2CH + C_6H_4 + Ph + C_5H_4N), 7.31 (1 H, d, $J = 16.1$ Hz, CH). Anal. Calcd (%) for $C_{26}H_{21}ClN_2 \cdot 3.25H_2O$: C, 68.56; H, 6.09; N, 6.15. Found: C, 68.59; H, 5.58; N, 6.29. *m/z*: 362 ($[M - Cl]^+$).

Synthesis of *N*-Phenyl-1,4-bis(*E*-2-(4-pyridyl)ethenyl)benzene Hexafluorophosphate, [Phbpvb$^+$]PF$_6$. [Phbpvb$^+$]Cl·3.25H$_2$O (500 mg, 1.10 mmol) was dissolved in methanol (20 mL), and aqueous NH_4PF_6 was added to produce a yellow precipitate, which was collected by filtration and washed with water. Purification was effected by several reprecipitations from DMF/water to afford a yellow solid. Yield: 747 mg (96%). δ_H(500 MHz, $(CD_3)_2SO$) 9.22 (2 H, d, $J = 6.9$ Hz, C_5H_4N), 9.14 (2 H, d, $J = 5.9$ Hz, C_5H_4N), 8.38 (2 H, d, $J = 6.9$ Hz, C_5H_4N), 8.21 (1 H, d, $J = 16.3$ Hz, CH), 7.89−7.70 (13 H, C_5H_4N + 2CH + C_6H_4, Ph), 7.47 (1 H, d, $J = 16.4$ Hz, CH). Anal. Calcd (%) for $C_{26}H_{21}F_6N_2P \cdot HPF_6 \cdot 3H_2O$: C; 44.21, H; 3.99, N; 3.97. Found: C, 43.98; H, 3.27; N, 4.63. *m/z*: 362 ($[M - PF_6]^+$). Orange shards suitable for X-ray crystallography were grown via slow diffusion of diethyl ether vapor into an acetonitrile/DMF solution. Anal. Calcd (%) for $C_{26}H_{21}F_6N_2P \cdot 0.5HPF_6 \cdot DMF$: C, 53.38; H, 4.40; N, 6.44. Found: C, 53.05; H, 4.42; N, 6.35.

Synthesis of *N*-(2-Pyrimidyl)-1,4-bis(*E*-2-(4-pyridyl)ethenyl)-benzene Hexafluorophosphate, [Pymbpvb$^+$]PF$_6$. This compound was prepared in a fashion identical to [Phbpvb$^+$]Cl by using [Pympic$^+$]$PF_6 \cdot 0.06C_4H_{10}O$ (154 mg, 0.479 mmol) in place of [Phpic$^+$]Cl·1.25H$_2$O. Purification of the brown solid was achieved by several reprecipitations from acetone/diethyl ether. Yield: 132 mg (58%). δ_H(300 MHz, $(CD_3)_2SO$), 9.84 (2 H, d, $J = 6.6$ Hz, C_5H_4N), 9.17 (2 H, d, $J = 4.8$ Hz, C_5H_4N), 8.56 (2 H, d, $J = 4.8$ Hz, $C_4H_3N_2$), 8.36 (2 H, d, $J = 6.9$ Hz, C_5H_4N), 8.35 (1 H, d, $J = 16.5$ Hz, CH), 7.88−7.72 (6 H, C_6H_4 + CH + $C_4H_3N_2$), 7.62−7.55 (3 H, C_5H_4N + CH), 7.52 (1 H, d, $J = 16.2$ Hz, CH). Anal. Calcd (%) for $C_{24}H_{19}F_6N_4P \cdot 2.5H_2O$: C, 52.09; H, 4.37; N, 10.12. Found: C, 52.35; H, 4.08; N, 9.67. *m/z*: 363 ($[M - PF_6]^+$).

Synthesis of *trans*-[Ru^{II}Cl(pdma)$_2$(bpvb)][PF$_6$]$_2$ (1). A solution of *trans*-$[Ru^{II}Cl(pdma)_2(NO)][PF_6]_2$ (125 mg, 0.122 mmol) and NaN_3 (8.1 mg, 0.125 mmol) in acetone (10 mL) was stirred at room temperature for 2 h. Butan-2-one (10 mL) and bpvb (179 mg, 0.629 mmol) were added, and the acetone was removed in vacuo. The solution was heated under reflux for 4 h, then cooled to room temperature. Diethyl ether was added, affording a dark orange precipitate which was collected by filtration and washed with diethyl ether. Purification was effected by precipitation from acetone/aqueous NH_4PF_6 followed by three reprecipitations from acetone/diethyl ether to afford a red solid. Yield: 32 mg (23%). δ_H(300 MHz, $(CD_3)_2CO$) 8.63 (2 H, d, $J = 5.4$ Hz, C_5H_4N), 8.29 (4 H, m, $C_6H_4(AsMe_2)_2$), 7.92 (4 H, m, $C_6H_4(AsMe_2)_2$), 7.86 (2 H, d, $J = 6.5$ Hz, C_5H_4N), 7.76−7.64 (5 H, CH + C_6H_4), 7.41−7.34 (4 H, 2CH + C_5H_4N), 7.11−7.01 (3 H, CH + C_5H_4N), 1.90 (12 H, s, 4AsMe), 1.73 (12 H, s, 4AsMe). Anal. Calcd (%) for $C_{40}H_{48}As_4ClF_6N_2PRu \cdot H_2O$: C, 41.56; H, 4.36; N, 2.42. Found: C, 41.50; H, 4.20; N, 2.43. *m/z*: 993 ($[M - PF_6]^+$).

Synthesis of *trans*-[Ru^{II}Cl(pdma)$_2$(Mebpvb$^+$)][PF$_6$]$_2$ (2). A solution of **1**·H$_2$O (32 mg, 0.028 mmol) in DMF (1.5 mL) and methyl iodide (0.4 mL) was stirred at room temperature for 24 h. The excess methyl iodide was removed in vacuo, and addition of aqueous NH_4PF_6 to the dark red solution gave a red precipitate, which was collected by filtration, washed with water, and dried. Purification was effected by reprecipitation from acetone/diethyl ether to afford a red solid. Yield: 19 mg (51%). δ_H(300 MHz, $(CD_3)_2CO$) 8.91 (2 H, d, $J = 6.9$ Hz, C_5H_4N), 8.34−8.27 (6 H, $C_6H_4(AsMe_2)_2$ + C_5H_4N), 8.21 (1 H, d, $J = 16.4$ Hz, CH), 7.85 (4 H, m, $C_6H_4(AsMe_2)_2$), 7.78 (2 H, d, $J = 8.5$ Hz, C_6H_4), 7.65 (2 H, d, $J = 8.5$ Hz, C_6H_4), 7.61−7.43 (4 H, 2CH + C_5H_4N), 7.23−7.14 (3 H, C_5H_4N + CH), 4.55 (3 H, s, Me), 1.91 (12 H, s, 4AsMe), 1.80 (12 H, s, 4AsMe). Anal. Calcd (%) for $C_{41}H_{51}As_4ClF_{12}N_2P_2Ru \cdot 2H_2O$: C, 36.91; H, 4.16; N, 2.10. Found: C, 36.92; H, 3.97; N, 2.09. *m/z*: 504 ($[M - PF_6]^{2+}$). Red slabs suitable for X-ray crystallography were grown via slow diffusion of diethyl ether vapor into an acetonitrile solution.

Synthesis of *trans*-[Ru^{II}Cl(pdma)$_2$(Phbpvb$^+$)][PF$_6$]$_2$ (3). This compound was prepared and purified in a fashion identical to **1** by using [Phbpvb$^+$]$PF_6 \cdot HPF_6 \cdot 3H_2O$ (94 mg, 0. 133 mmol) in place of bpvb to afford a red solid. Yield: 39 mg (24%). δ_H(300 MHz, $(CD_3)_2CO$) 9.20 (2 H, d, $J = 7.2$ Hz, C_5H_4N), 8.46 (2 H, d, $J = 7.0$ Hz, C_5H_4N), 8.32 (4 H, m, $C_6H_4(AsMe_2)_2$), 8.16 (1 H, d, $J = 16.3$ Hz, CH), 7.92 (2 H, m, C_6H_4), 7.89 (4 H, m, $C_6H_4(AsMe_2)_2$), 7.81−7.66 (8 H, C_6H_4 + CH + Ph), 7.56 (2 H, d, $J = 6.7$ Hz, C_5H_4N), 7.46 (1 H, d, $J = 16.3$ Hz, CH), 7.24−7.15 (3 H, C_5H_4N + CH), 1.90 (12 H, s, 4AsMe), 1.80 (12 H, s, 4AsMe). Anal. Calcd (%) for $C_{46}H_{53}As_4ClF_{12}N_2P_2Ru$: C, 40.62; H, 3.93; N, 2.06. Found: C, 40.53; H, 3.47; N, 2.02. *m/z*: 534 ($[M - PF_6]^{2+}$). Red needles suitable for X-ray crystallography were grown via slow diffusion of diethyl ether vapor into an acetonitrile solution.

Synthesis of *trans*-[Ru^{II}Cl(pdma)$_2$(Pymbpvb$^+$)][PF$_6$]$_2$ (4). This compound was prepared and purified in a fashion identical to **1** by using [Pymbpvb$^+$]$PF_6 \cdot 2.5H_2O$ (95 mg, 0.172 mmol) in place of bpvb to afford a red/brown solid. Yield: 37 mg (21%). δ_H(300 MHz, $(CD_3)_2CO$) 10.05 (2 H, d, $J = 7.3$ Hz, C_5H_4N), 9.22 (2 H, d, $J = 4.8$ Hz, $C_4H_3N_2$), 8.53 (2 H, d, $J = 7.3$ Hz, C_5H_4N), 8.33 (4 H, m, $C_6H_4(AsMe_2)_2$), 8.28 (1 H, d, $J = 16.7$ Hz, CH), 7.96 (1 H, t, $J = 4.8$ Hz, $C_4H_3N_2$), 7.89−7.84 (6 H, $C_6H_4(AsMe_2)_2$ + C_6H_4), 7.79 (1 H, $J = 16.3$ Hz, CH), 7.70 (2 H, d, $J = 8.4$ Hz, C_6H_4), 7.58 (2 H, d, $J = 6.7$ Hz, C_5H_4N), 7.48 (1 H, d, $J = 16.4$ Hz, CH), 7.25−7.18 (3 H, C_5H_4N + CH), 1.90 (12 H, s, 4AsMe), 1.81 (12 H, s, 4AsMe). Anal. Calcd (%) for $C_{44}H_{51}As_4ClF_{12}N_4P_2Ru \cdot 3H_2O$: C, 37.32; H, 4.06; N, 3.96. Found: C, 36.91; H, 3.53; N, 3.96. *m/z*: 536 ($[M - PF_6]^{2+}$).

X-ray Crystallography. The crystals chosen for diffraction studies had the following approximate dimensions and appearances: 0.18 × 0.16 × 0.04 mm^3, orange shard ([Phbpvb$^+$]$PF_6 \cdot 0.5HPF_6 \cdot DMF$); 0.42 × 0.30 × 0.07 mm^3, dark red slab (**2**); 0.76 × 0.18 × 0.03 mm^3, dark red blade (**3**). Data were collected on a Nonius Kappa CCD area-detector diffractometer controlled by the Collect software package.[16] The data were processed by Denzo[17] and corrected for absorption by using SADABS.[18] The structures were solved by direct methods and refined by full-matrix least-squares on all F_0^2 data using SHELXS-97[19] and SHELXL-97.[20] All non-hydrogen atoms were refined anisotropically with hydrogen atoms included in idealized positions with thermal parameters riding on those of the parent atom. The crystal of [Phbpvb$^+$]$PF_6 \cdot 0.5HPF_6$ contains a molecule of highly disordered solvent (DMF) in the asymmetric unit, while the crystals of **2** and **3** contain unspecified

(16) Hooft, R. *Collect, Data collection software*; Nonius BV: Delft, The Netherlands, 1998.
(17) Otwinowski, Z.; Minor, W. *Methods Enzymol.* **1997**, *276*, 307.
(18) Sheldrick, G. M. *SADABS* (Version 2.10); Bruker AXS, Inc.; Madison: WI, 2003.
(19) Sheldrick, G. M. *Acta Crystallogr. Sect. A* **1990**, *46*, 467.
(20) Sheldrick, G. M. *SHELXL 97, Program for Crystal Structure Refinement*; University of Göttingen: Göttingen, Germany, 1997.

Table 1. Crystallographic Data and Refinement Details for the Salts [Phbpvb$^+$]PF_6·0.5HPF_6, **2**, and **3**

	[Phbpvb$^+$]PF_6·0.5HPF_6	**2**	**3**
empirical formula	$C_{52}H_{43}F_{18}N_4P_3$	$C_{41}H_{51}As_4ClF_{12}N_2P_2Ru$	$C_{46}H_{53}As_4ClF_{12}N_2P_2Ru$
fw	1158.81	1297.98	1360.04
cryst syst	monoclinic	monoclinic	monoclinic
space group	*C*2/*c*	$P2_1/n$	$P2_1/n$
a/Å	42.215(8)	9.5973(12)	9.345(2)
b/Å	10.309(2)	42.589(5)	53.743(9)
c/Å	14.107(3)	15.082(2)	25.264(4)
β/deg	105.77(3)	105.201(10)	98.056(16)
U/Å^3	5908(2)	5948.7(13)	12562(4)
Z	4	4	8
T/K	120(2)	120(2)	120(2)
μ/mm^{-1}	0.194	2.634	2.499
reflns collected	29 037	25 450	46 744
independent reflns (R_{int})	5196 (0.1072)	7097 (0.0635)	16 036 (0.0974)
GOF on F^2	1.022	1.176	1.048
final R1, wR2 [$I > 2\sigma(I)$]	0.1162, 0.2875	0.0934, 0.2757	0.1044, 0.2636
final R1, wR2 (all data)	0.2121, 0.3356	0.1445, 0.3231	0.2371, 0.3131

[a] The structures were refined on F_o^2 using all data; the values of R1 are given for comparison with older refinements based on F_o with a typical threshold of $F_o > 4\sigma(F_o)$.

amounts of unrefinable solvent (acetonitrile); all disordered solvent was removed by using the SQUEEZE procedure.[21] In [Phbpvb$^+$]-PF_6·0.5HPF_6, one of the PF_6^- anions is disordered over two sites (and over a symmetry operation). There is a hydrogen atom between two pyridine nitrogen atoms related by a symmetry operation forming a strong hydrogen bond. Because it was not possible to accurately locate this hydrogen atom, it was fixed to the nitrogen with half occupancy to best model the situation. In **2**, the two PF_6^- anions are disordered over two sites, while **3** contains two independent complex cations that are also disordered over two sites. Crystallographic data and refinement details are presented in Table 1.

Stark Spectroscopy. The Stark apparatus, experimental methods, and data analysis procedure were exactly as previously reported,[22] with the only modification being that a Xe arc lamp was used as the light source instead of a W filament bulb. Butyronitrile was used as the glassing medium, for which the local field correction, f_{int}, is estimated as 1.33.[22] The Stark spectrum for each compound was measured a minimum of three times using different field strengths, and the signal was always found to be quadratic in the applied field. A two-state analysis of the ICT transition gives

$$\Delta\mu_{ab}^2 = \Delta\mu_{12}^2 + 4\mu_{12}^2 \quad (1)$$

where $\Delta\mu_{ab}$ is the dipole moment difference between the diabatic states, $\Delta\mu_{12}$ is the observed (adiabatic) dipole moment difference, and μ_{12} is the transition dipole moment. Analysis of the Stark spectra in terms of the Liptay treatment[4] affords $\Delta\mu_{12}$, and μ_{12} can be determined from the oscillator strength, f_{os}, of the transition by

$$|\mu_{12}| = [f_{os}/(1.08 \times 10^{-5} E_{max})]^{1/2} \quad (2)$$

where E_{max} is the energy of the ICT maximum (in wavenumbers). The degree of delocalization, c_b^2, and electronic coupling matrix element, H_{ab}, for the diabatic states are given by

$$c_b^2 = \frac{1}{2}\left[1 - \left(\frac{\Delta\mu_{12}^2}{\Delta\mu_{12}^2 + 4\mu_{12}^2}\right)^{1/2}\right] \quad (3)$$

$$|H_{ab}| = \left|\frac{E_{max}(\mu_{12})}{\Delta\mu_{ab}}\right| \quad (4)$$

If the hyperpolarizability tensor β_0 has only nonzero elements along the ICT direction, then this quantity is given by

$$\beta_0 = \frac{3\Delta\mu_{12}(\mu_{12})^2}{(E_{max})^2} \quad (5)$$

A relative error of ±20% is estimated for the β_0 values derived from the Stark data and using eq 5, while experimental errors of ±10% are estimated for μ_{12}, $\Delta\mu_{12}$, and $\Delta\mu_{ab}$, ±15% for H_{ab}, and ±50% for c_b^2.

Results and Discussion

Synthetic Studies. Previously studied Ru^{II} ammine complexes of the ligand Mebpvb$^+$ display relatively large contributions to β of $\pi \rightarrow \pi^*$ intraligand charge-transfer (ILCT) (as well as MLCT) transitions, and show increased optical transparencies when compared with related polyenyl chromophores.[5a] We have also investigated some *trans*-{Ru^{II}-$Cl(pdma)_2$}$^+$ complexes,[23] and the new complex salts **2**−**4** (Figure 1) were designed to probe the effects on the optical properties of extending the π-conjugation by incorporating a 1,4-phenylene unit into such pdma-containing chromophores.

The complex in **1** (Figure 1) was prepared via reaction of the neutral pro-ligand bpvb with the sodium azide-treated complex precursor *trans*-[$Ru^{II}Cl(pdma)_2(NO)$]$^{2+}$,[12] and **3** and **4** were prepared similarly but using the pro-ligand salts [Phbpvb$^+$]PF_6 and [Pymbpvb$^+$]PF_6 (Figure 1), respectively. The complex in **2** was synthesized via treatment of **1** with methyl iodide in DMF. Such a synthetic approach is not suitable for complexes of related *N*-aryl ligands, so the species Phbpvb$^+$ and Pymbpvb$^+$ were synthesized by Knoevenagel-type condensation reactions between FEP (Figure 1) and the corresponding picolinium salt using pyridine as the base. The salt [Phbpvb$^+$]PF_6 was isolated as its HPF_6

(21) van der Sluis, P.; Spek, A. L. *Acta Crystallogr. Sect A* **1990**, *46*, 194.
(22) (a) Shin, Y. K.; Brunschwig, B. S.; Creutz, C.; Sutin, N. *J. Phys. Chem.* **1996**, *100*, 8157. (b) Coe, B. J.; Harris, J. A.; Brunschwig, B. S. *J. Phys. Chem. A* **2002**, *106*, 897.
(23) Coe, B. J.; Harries, J. L.; Harris, J. A.; Brunschwig, B. S.; Coles, S. J.; Light, M. E.; Hursthouse, M. B. *Dalton Trans*. **2004**, 2935.

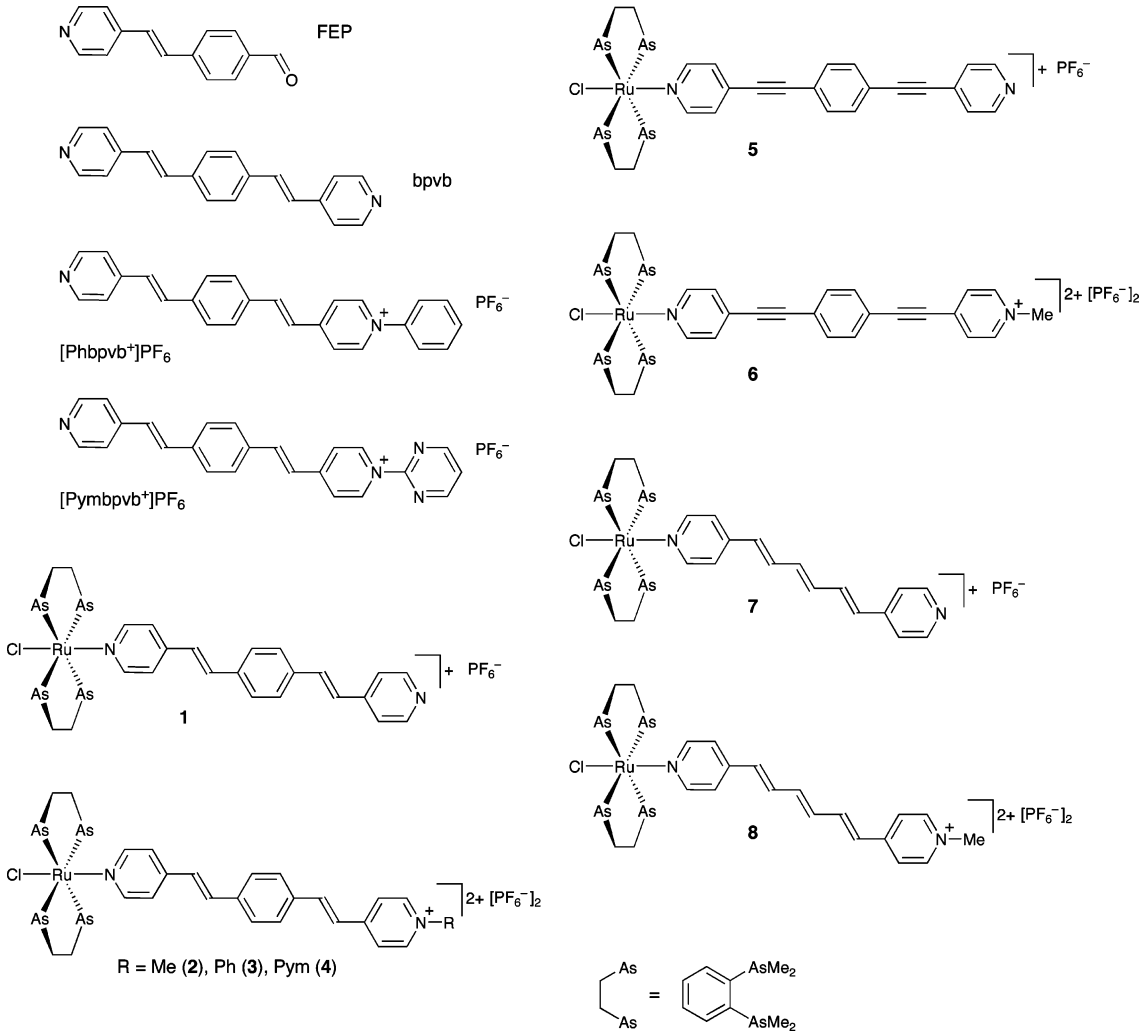

Figure 1. Chemical structures of FEP and the pro-ligand salts and Ru^{II} complex salts investigated.

adduct. All of the new compounds show diagnostic ^{1}H NMR spectra, and mass spectra and elemental analyses provide further confirmation of identity and purity.

Electronic Spectroscopy Studies. The UV−visible absorption spectra of salts **1**−**4** have been measured in acetonitrile, and the results are presented in Table 2, together with data for the previously reported related compounds **5**−**8** [bpeb = 1,4-bis(4-pyridylethynyl)benzene, bph = *E*,*E*,*E*-1,6-bis(4-pyridyl)hexa-1,3,5-triene].[5d,23] These spectra feature intense absorptions in the UV region due to ILCT transitions, together with intense, broad $d(Ru^{II}) \rightarrow \pi^*(L_A)$ (L_A = pyridyl ligand) visible MLCT bands.

As expected, methylation of the uncoordinated pyridyl nitrogen in **1** to afford **2** produces a red-shift in the MLCT band, accompanied by a decrease in intensity. An almost 3-fold larger corresponding decrease in the energy of the ILCT band is observed. Within the pyridinium series **2**−**4**, both the ILCT and MLCT bands red-shift steadily on moving from R = Me to Pym (Figure 2). This trend is consistent with previous observations with related complexes,[24] and can be ascribed to destabilization of the L_A-based LUMO as the pyridinium unit becomes more electron deficient, as confirmed by cyclic voltammetric measurements (see later). The intensities of both the ILCT and MLCT absorptions also appear to increase with the π-acceptor strength of L_A, although the strong overlapping of the bands means that this apparent trend may not be real.

The MLCT bands of **2** and **6** have very similar energies and intensities, showing that replacing the *E*-ethenyl units with ethynyl groups has no significant effects. However, the ILCT absorption spectra of these two compounds are quite different. In contrast, for the corresponding unmethylated complex salts (**1** and **5**), changing the structure of the bridge affects the energy and intensity of both the MLCT and ILCT bands, but the effects on the latter absorption are more significant. When compared with the complex in **7**, which features an extra *E*-ethenyl unit in place of the 1,4-phenylene bridge, the MLCT and ILCT bands of **1** are both blue-shifted by ca. 0.1 eV. Larger corresponding shifts of ca. 0.2 eV are observed when moving from the *N*-methylated complex in **2** to that in **8**, an observation that is consistent with published data for related Ru^{II} ammine complexes.[5a]

(24) (a) Coe, B. J.; Harris, J. A.; Asselberghs, I.; Persoons, A.; Jeffery, J. C.; Rees, L. H.; Gelbrich, T.; Hursthouse, M. B. *J. Chem. Soc., Dalton Trans*. **1999**, 3617. (b) Coe, B. J.; Beyer, T.; Jeffery, J. C.; Coles, S. J.; Gelbrich, T.; Hursthouse, M. B.; Light, M. E. *J. Chem. Soc., Dalton Trans*. **2000**, 797.

Table 2. UV−Visible and Electrochemical Data for Complex Salts **1**−**8** in Acetonitrile

salt	λ_{max},[a] nm (ϵ, M^{-1} cm^{-1})	E_{max},[a] eV	assignment	E, V vs Ag/AgCl (ΔE_p, mV)[b] $E_{1/2}[Ru^{III/II}]$	$E_{1/2}[L_A^{+/0}]$ or E_{pc}[c]
trans-$[Ru^{II}Cl(pdma)_2(bpvb)]PF_6$ (**1**)	432 (20 300)	2.87	d → π^*	1.05 (80)	−1.40 (100)
	350 (51 700)	3.54	$\pi \rightarrow \pi^*$		
trans-$[Ru^{II}Cl(pdma)_2(Mebpvb^+)][PF_6]_2$ (**2**)	444 (15 600)	2.79	d → π^*	1.06 (65)	−0.95
	372 (34 400)	3.33	$\pi \rightarrow \pi^*$		−1.63
trans-$[Ru^{II}Cl(pdma)_2(Phbpvb^+)][PF_6]_2$ (**3**)	460 (22 300)	2.70	d → π^*	1.06 (60)	−0.76
	398 (36 700)	3.12	$\pi \rightarrow \pi^*$		−1.60
trans-$[Ru^{II}Cl(pdma)_2(Pymbpvb^+)][PF_6]_2$ (**4**)	474sh (25 600)	2.62	d → π^*	1.05 (70)	−0.55
	416 (40 100)	2.98	$\pi \rightarrow \pi^*$		−1.57
trans-$[Ru^{II}Cl(pdma)_2(bpeb)]PF_6$[d] (**5**)	438 (15 000)	2.83	d → π^*	1.10 (75)	−1.40 (95)
	320 (39 200)	3.88	$\pi \rightarrow \pi^*$		
trans-$[Ru^{II}Cl(pdma)_2(Mebpeb^+)][PF_6]_2$[d] (**6**)	446 (15 500)	2.78	d → π^*	1.11 (75)	−0.89
	354 (37 400)	3.50	$\pi \rightarrow \pi^*$		−1.56
	344sh (35 900)	3.60	$\pi \rightarrow \pi^*$		
	276 (24 100)	4.49	$\pi \rightarrow \pi^*$		
trans-$[Ru^{II}Cl(pdma)_2(bph)]PF_6$[e] (**7**)	446 (18 800)	2.78	d → π^*	1.06 (90)	−1.07
	362 (37 300)	3.43	$\pi \rightarrow \pi^*$		
trans-$[Ru^{II}Cl(pdma)_2(Mebph^+)][PF_6]_2$[e] (**8**)	472 (15 000)	2.58	d → π^*	1.07 (110)	−0.80
	394 (26 800)	3.15	$\pi \rightarrow \pi^*$		

[a] Solutions of ca. 3−8 × 10^{-5} M. [b] Solutions of ca. 10^{-3} M in analyte and 0.1 M in $[NBu^n_4]PF_6$ at a Pt disk working electrode with a scan rate of 200 mV s^{-1}. Ferrocene internal reference $E_{1/2}$ = 0.43 V and ΔE_p = 60−110 mV. [c] For an irreversible reduction process. [d] Reference 5d. [e] Reference 23.

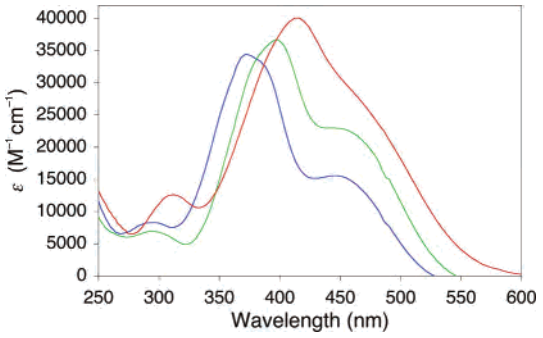

Figure 2. UV−visible absorption spectra of complex salts **2** (blue), **3** (green), and **4** (red) in acetonitrile at 295 K.

Electrochemical Studies. The new complex salts **1**−**4** were studied by cyclic voltammetry in acetonitrile, and the results are presented in Table 2, together with data for the previously reported related compounds **5**−**8**.[5d,23] All of the complexes show reversible $Ru^{III/II}$ oxidation waves, together with generally irreversible pyridyl ligand-based reduction processes, with the exceptions of **1** and **5** for which the reductions are reversible.

Methylation of the uncoordinated pyridyl nitrogen in **1** to form **2** stabilizes the L_A-based LUMO, as evidenced by an increased first reduction potential. Since the $Ru^{III/II}$ $E_{1/2}$ value is unchanged by methylation, the accompanying red-shift of the MLCT absorption band can be attributed solely to a decrease in the LUMO energy, with the energy of the Ru-based HOMO remaining constant. As noted previously,[5d,23] similar effects are observed in the pairs **5**/**6** and **7**/**8**. Within the series **2**−**4**, $E_{1/2}[Ru^{III/II}]$ remains constant while the first ligand-based reduction potential increases steadily, indicating that the corresponding red-shifting of the MLCT band is again attributable only to stabilization of the L_A-based LUMO. The ethenyl-containing complexes in **1**, **2**, **7**, and **8** display slightly lower $E_{1/2}[Ru^{III/II}]$ values when compared with their ethynyl counterparts in **5** and **6**, an observation that can be ascribed to the lower net electron-donating abilities of the L^A ligands in the latter species.

Crystallographic Studies. Single-crystal X-ray structures have been obtained for the pro-ligand salt $[Phbpvb^+]PF_6 \cdot 0.5HPF_6$ and for the complex salts **2** and **3**, and representations of the molecular structures are shown in Figures 3−5. Selected crystallographic and refinement details are shown in Table 1, and selected bond lengths and angles are shown in Tables 3 and 4. These structures are not of the highest quality due to the presence of disordered solvents and the sensitivity of the crystals toward solvent loss, so all bond lengths and angles must be treated with care.

The twisting between the aryl rings within the conjugated pyridinium-substituted systems is somewhat variable, as shown by the dihedral angles given in Table 5, but the bpvb units are reasonably planar due to their highly π-conjugated nature. Unfortunately, all of these materials adopt centrosymmetric space groups, so no significant bulk NLO behavior is to be expected. There is, however, a reasonable likelihood that metathesis of the PF_6^- anions in **2** and **3** will produce different packing arrangements of the constituent complex chromophores that may then show NLO activity. Although it is not possible to reliably predict how changing the counteranions will affect crystal packing structures, commonly used species such as $MeC_6H_4SO_3^-$ (tosylate) or BPh_4^- (tetraphenylborate) are attractive candidates due to their widely different steric properties when compared with the small pseudo-spherical PF_6^- anion. Exploiting a chiral anion such as (+)-10-camphorsulfonate should further encourage the formation of favorable non-centrosymmetric structures, and the use of an anion that also shows NLO activity, for example a $\{Fe^{II}(CN)_5\}^{3-}$ complex,[7] is another intriguing possibility.

Stark Spectroscopic Studies. Measurement of the molecular NLO responses of the complex chromophores in **2**−**4** presents some challenges. Resonantly enhanced β values for ionic chromophores are generally obtained via hyper-Rayleigh scattering experiments[3] and may be corrected for

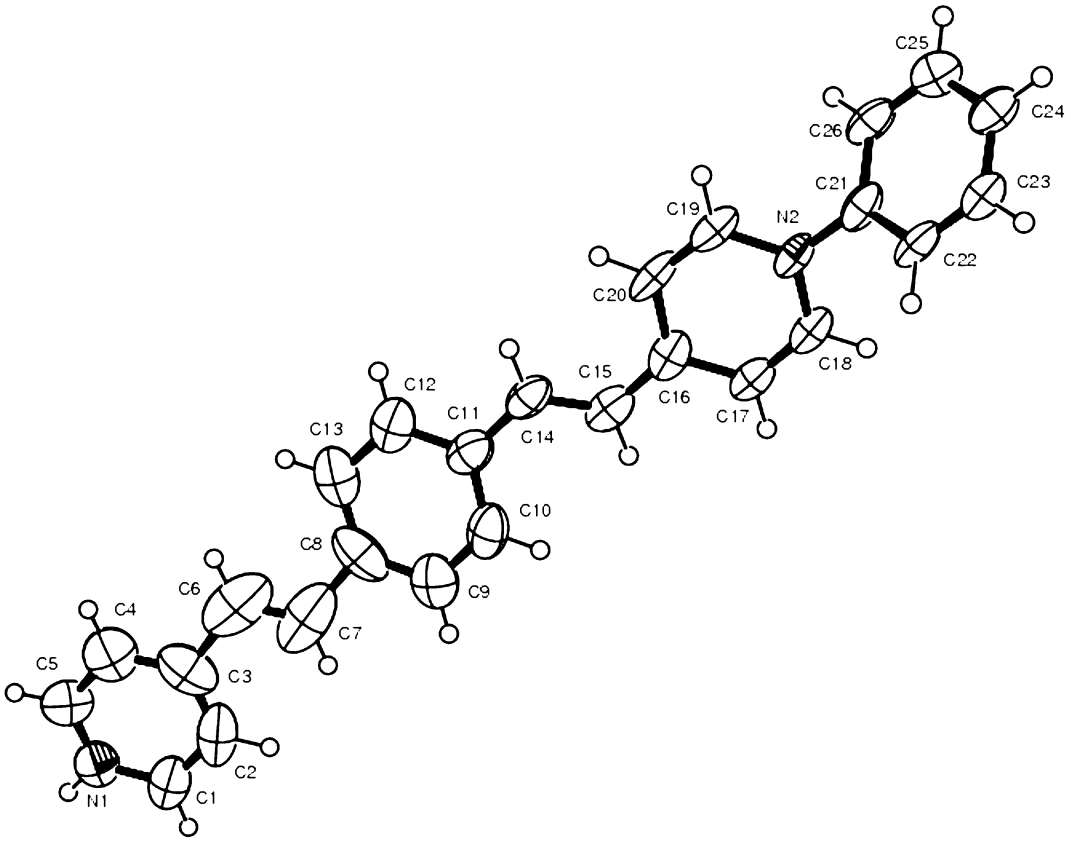

Figure 3. Structural representation of the protonated pro-ligand cation in the salt $[Phbpvb^{+}]PF_6 \cdot 0.5HPF_6$ (50% probability ellipsoids).

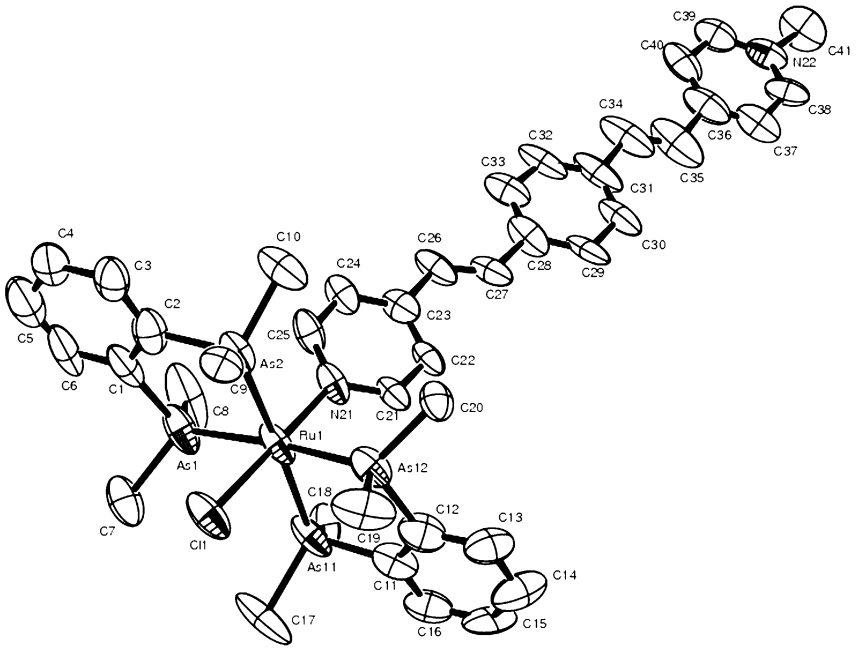

Figure 4. Structural representation of the complex cation in salt **2** (50% probability ellipsoids).

dispersion by using a simple two-state model,[8] provided that a single ICT process dominates the β response. However, this approach to determining β_0 values is not feasible for chromophores with strongly overlapping low-energy ICT bands, such as **2**−**4** (Figure 2). We have found that Stark spectroscopy is very valuable for probing the NLO and related properties of a range of metal complexes[5,7,22b,23] and have now also applied this technique to **2**−**4**. Besides our own previous studies, only relatively few other reports have described the use of this method to determine β responses.[25] In the present instance, Stark spectroscopy becomes particularly invaluable as the only viable approach to obtain

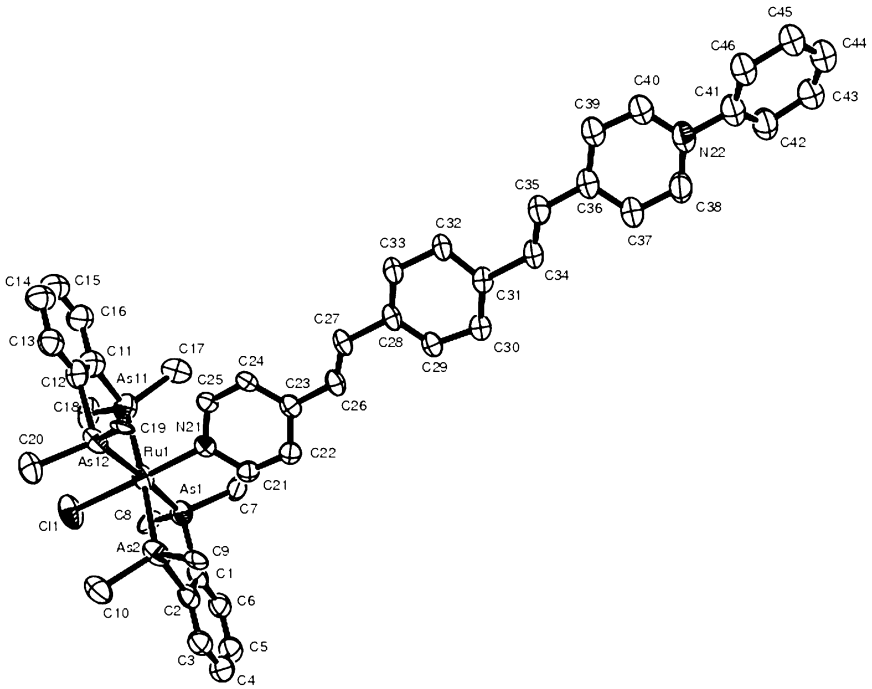

Figure 5. Structural representation of one of the two independent complex cations in salt **3** (50% probability ellipsoids).

Table 3. Selected Interatomic Distances (Å) and Angles (deg) for $[Phbpvb^+]PF_6 \cdot 0.5HPF_6$

C3−C6	1.627(12)	C11−C14	1.454(9)
C6−C7	1.222(11)	C14−C15	1.357(8)
C7−C8	1.583(12)	C15−C16	1.426(8)
C7−C6−C3	115.9(10)	C15−C14−C11	125.4(6)
C6−C7−C8	118.1(10)	C14−C15−C16	125.7(6)

Table 4. Selected Interatomic Distances (Å) and Angles (deg) for Complex Salts **2** and **3** (One Cation Only)

	2	**3**
Cl1−Ru1	2.443(3)	2.445(9)
Ru1−N21	2.142(10)	2.108(12)
Ru1−As1	2.4197(17)	2.405(7)
Ru1−As11	2.4141(19)	2.412(7)
Ru1−As12	2.4118(17)	2.413(7)
Ru1−As2	2.4134(19)	2.407(7)
N21−Ru1−As1	94.5(3)	95.1(6)
N21−Ru1−As11	91.4(3)	91.0(6)
As1−Ru1−As11	95.01(6)	93.5(3)
N21−Ru1−As12	91.8(3)	90.1(6)
As1−Ru1−As12	173.61(6)	174.4(5)
N21−Ru1−As2	93.4(3)	93.5(6)
As1−Ru1−As2	85.29(6)	84.9(3)
As11−Ru1−As2	175.19(6)	175.4(5)
As12−Ru1−As2	94.91(6)	96.8(3)
N21−Ru−Cl1	179.1(3)	178.4(7)
As1−Ru1−Cl1	84.60(10)	86.4(5)
As11−Ru1−Cl1	88.64(10)	88.4(4)
As12−Ru1−Cl1	89.04(10)	88.3(5)
As2−Ru1−Cl1	86.61(10)	87.1(4)

meaningful β_0 values. The samples were studied as butyronitrile glasses at 77 K, and the results are presented in Table 6, together with data for the previously reported related compounds **6** and **8**.[5d,23] Representative absorption and Stark spectra for the MLCT bands of **2**−**4** are shown in Figure 6.

The MLCT bands of these complex salts generally show reasonably large red-shifts (ca. 0.1−0.2 eV) when moving from acetonitrile solutions at 295 K to butyronitrile glasses at 77 K, as observed in various related compounds.[5,22b,23] However, salt **4** provides a notable exception and shows a corresponding blue-shift. Hence, although the MLCT band red-shifts as the acceptor strength of L_A increases on moving along the series **2**−**4** at 295 K, this trend is not maintained at 77 K since the MLCT band shows a blue-shift on moving from **3** to **4**. However, it should be noted that due to the strong overlap of the MLCT and ILCT bands in **4**, the quoted λ_{max} and E_{max} values should be viewed only as estimates.

On moving along the series **2**−**4**, no significant changes are observed in μ_{12} or f_{os}, but both $\Delta\mu_{12}$ and $\Delta\mu_{ab}$ increase steadily, with $\Delta\mu_{ab}$ being larger in every instance. Steady decreases in both H_{ab} and c_b^2 are observed as the electron-accepting ability of L_A increases; as these quantities are related to the degree of orbital overlap, it is clear that the D−A electronic coupling decreases on moving along the series from **2** to **4**. The derived values for β_0 increase as the L_A acceptor strength increases on moving from **2** to **3**, but replacing the Ph group in **3** with Pym in **4** causes no significant change in the NLO response. Previous Stark studies with Ru^{II} ammine or arsine complexes, as well as with Fe^{II} cyanides, have invariably shown that β_0 increases by as much as 2-fold on moving from a *N*-phenylpyridinium to a *N*-(2-pyrimidyl)pyridinium A group.[7,22b,23] The surprising result in this instance can be rationalized by considering that **4** has an unexpectedly low apparent value for E_{max}, as discussed above.

(25) Selected examples: (a) Bublitz, G. U.; Ortiz, R.; Marder, S. R.; Boxer, S. G. *J. Am. Chem. Soc.* **1997**, *119*, 3365. (b) Wolff, J. J.; Längle, D.; Hillenbrand, D.; Wortmann, R.; Matschiner, R.; Glania, C.; Krämer, P. *Adv. Mater.* **1997**, *9*, 138. (c) Karki, L.; Vance, F. W.; Hupp, J. T.; LeCours, S. M.; Therien, M. J. *J. Am. Chem. Soc.* **1998**, *120*, 2606. (d) Vance, F. W.; Hupp, J. T. *J. Am. Chem. Soc.* **1999**, *121*, 4047. (e) Barlow, S.; Bunting, H. E.; Ringham, C.; Green, J. C.; Bublitz, G. U.; Boxer, S. G.; Perry, J. W.; Marder, S. R. *J. Am. Chem. Soc.* **1999**, *121*, 3715. (f) Wolff, J. J.; Siegler, F.; Matschiner, R.; Wortmann, R. *Angew. Chem., Int. Ed.* **2000**, *39*, 1436.

Table 5. Dihedral Angles (deg) for Salts [Phbpvb$^+$]PF_6·0.5HPF_6, **2** and **3** (Two Independent Cations)[a]

compound	py−Ph	Ph−pyr	pyr−Ph
[Phbpvb$^+$]PF_6·0.5HPF_6	13.05(0.16)	13.30(0.15)	50.89(0.15)
2	7.16(0.68)	2.29(0.73)	
3	1.39(2.21)/6.37(2.24)	13.07(1.93)/4.03(2.21)	42.35(1.62)/38.08(1.73)

[a] (py = pyridyl; pyr = pyridinium)

Table 6. MLCT Absorption and Stark Spectroscopic Data for Salts **2**−**4**, **6** and **8**

salt	λ_{max}[a] nm	λ_{max}[b] nm	E_{max}[b] eV	f_{os}[b]	μ_{12}[c] D	$\Delta\mu_{12}$[d] D	$\Delta\mu_{ab}$[e] D	c_b^2[f]	H_{ab}[g] cm^{-1}	β_0[h] 10^{-30} esu
2	444	471	2.63	0.4	6.4	18.8	22.8	0.09	6000	131
3	460	481	2.58	0.5	6.8	24.9	28.4	0.06	5000	203
4	474	464	2.67	0.4	6.3	31.0	33.4	0.04	4100	200
6[i]	446	472	2.63	0.3	5.4	23.2	25.7	0.05	4450	114
8[j]	472	501	2.48	1.0	10.5	22.2	30.6	0.14	6900	468

[a] In acetonitrile solutions at 295 K. [b] In butyronitrile glasses at 77 K. [c] Calculated from eq 2. [d] Calculated from $f_{int}\Delta\mu_{12}$ using $f_{int} = 1.33$. [e] Calculated from eq 1. [f] Calculated from eq 3. [g] Calculated from eq 4. [h] Calculated from eq 5. [i] Reference 5d. [j] Reference 23.

Replacement of the ethenyl units in **2** with ethynyl bonds (in **6**) causes slight decreases in both μ_{12} and f_{os}, but the two chromophores have similar MLCT energies. The values of $\Delta\mu_{12}$ and $\Delta\mu_{ab}$ are both larger for **6**, while **2** has larger values for both H_{ab} and c_b^2, attributable to more effective D−A electronic communication via the ethenyl bridges. However, the estimated β_0 responses of **2** and **6** are of a similar magnitude, and this observation can be ascribed to the effect of the smaller value of μ_{12} for **6** being offset by its larger $\Delta\mu_{12}$ value. Comparison of **2** with its *E*,*E*,*E*-1,6-hexa-1,3,5-trienyl analogue **8** reveals a much larger β_0 response for the latter (when considering only the MLCT bands) that is attributable to a decrease in E_{max} and increases in both μ_{12} and $\Delta\mu_{12}$.

Because the ILCT bands of complex salts **2**−**4** are so intense and close in energy to the MLCT bands, the overall NLO responses will feature significant contributions from both transitions. We have therefore also performed Stark measurements on the ILCT bands, and the resulting data are presented in Table 7. Representative absorption and Stark spectra for the ILCT bands of **2**−**4** are shown in Figure 7. Unfortunately, corresponding data are not available for the previously reported complex salts **6** or **8**.

Within the series **2**−**4**, μ_{12}, f_{os}, $\Delta\mu_{12}$, and $\Delta\mu_{ab}$ for the ILCT absorptions all increase and E_{max} decreases as the electron accepting ability of L_A increases. The μ_{12} values are larger than those of the MLCT absorptions in every instance, correlating with the ILCT transitions being more strongly allowed. However, the $\Delta\mu_{12}$ values of the ILCT bands are smaller by ca. 40% when compared with those of the MLCT absorptions. The derived β_0 values associated with the ILCT transitions increase steadily on moving from **2** to **4** because μ_{12} and $\Delta\mu_{12}$ increase while E_{max} decreases. Because the MLCT and ILCT transitions in these 1D dipolar complex chromophores are codirectional and lie along the same axis, their contributions to the total NLO response are additive. This is a very unusual situation since in the vast majority of complexes studied previously by ourselves and others the NLO responses are dominated by just one type of transition. MLCT transitions are typically the most important, but a number of tris-chelates are known in which the ILCT transitions dominate and are actually directionally opposed to the MLCT transitions (which therefore act to decrease the overall hyperpolarizability).[25d,26] Although certain ferrocenyl NLO chromophores also display putative ILCT and MLCT transitions that contribute to the β response,[25e,27] some controversy exists regarding the electronic structures of such complexes, and the two transitions cannot in any case be completely aligned due to the marked nonlinearity of the molecular structures.

The estimated total β_0 responses for **2**−**4**, obtained by addition of the contributions from the MLCT and ILCT transitions, are shown in Table 7. The contribution of the ILCT transition to the overall NLO response increases steadily on moving along the series from **2** to **4**, reaching as much as ca. 45% for **4**. However, the unexpectedly low E_{max} and β_0 values associated with the MLCT transition for **4** may mean that the ILCT contribution in this case is actually less than that implied by the data presented here. Nevertheless, **2**−**4** evidently exhibit very large total β_0 values, especially considering that their visible absorptions are at relatively high energy. We have previously described Ru^{II} ammine chromophores with β_0 values of over 600×10^{-30} esu,[5a] but these species absorb strongly across much of the visible region and into the near-infrared. These new pdma-containing chromophores are therefore promising candidates for further study.

One of the motivations for the present investigation was the observation that Ru^{II} ammine complexes of the extended ligand Mebpvb$^+$ exhibit large NLO responses together with increased visible transparency, when compared with related complexes of the polyenyl ligand Mebph$^+$.[5a] However, although **2** does show a considerable gain in visible transparency when compared with **8** (the absorption cutoff for **2** is ca. 90 nm lower in acetonitrile at 295 K), the estimated NLO response is more than twice as large for **8**. Furthermore, the quoted value for **8** was obtained without considering the contribution of the ILCT transition,[23] so the actual difference in NLO activity between these two chromophores must be even larger than 2-fold. In marked contrast, Stark data for related Ru^{II} ammine complexes of the ligands Mebpvb$^+$ and Mebph$^+$ reveal decreases in the total β_0 response of only ca. 15−25% on replacing the central *E*-ethenyl bond with a

(26) Selected examples: (a) Dhenaut, C.; Ledoux, I.; Samuel, I. D. W.; Zyss, J.; Bourgault, M.; Le Bozec, H. *Nature* **1995**, *374*, 339. (b) Maury, O.; Viau, L.; Sénéchal, K.; Corre, B.; Guégan, J.-P.; Renouard, T.; Ledoux, I.; Zyss, J.; Le Bozec, H. *Chem.—Eur. J.* **2004**, *10*, 4454. (c) Maury, O.; Le, Bozec, H. *Acc. Chem. Res.* **2005**, *38*, 691.

(27) Selected examples: (a) Calabrese, J. C.; Cheng, L.-T.; Green, J. C.; Marder, S. R.; Tam, W. *J. Am. Chem. Soc.* **1991**, *113*, 7227. (b) Kanis, D. R.; Ratner, M. A.; Marks, T. J. *J. Am. Chem. Soc.* **1992**, *114*, 10338.

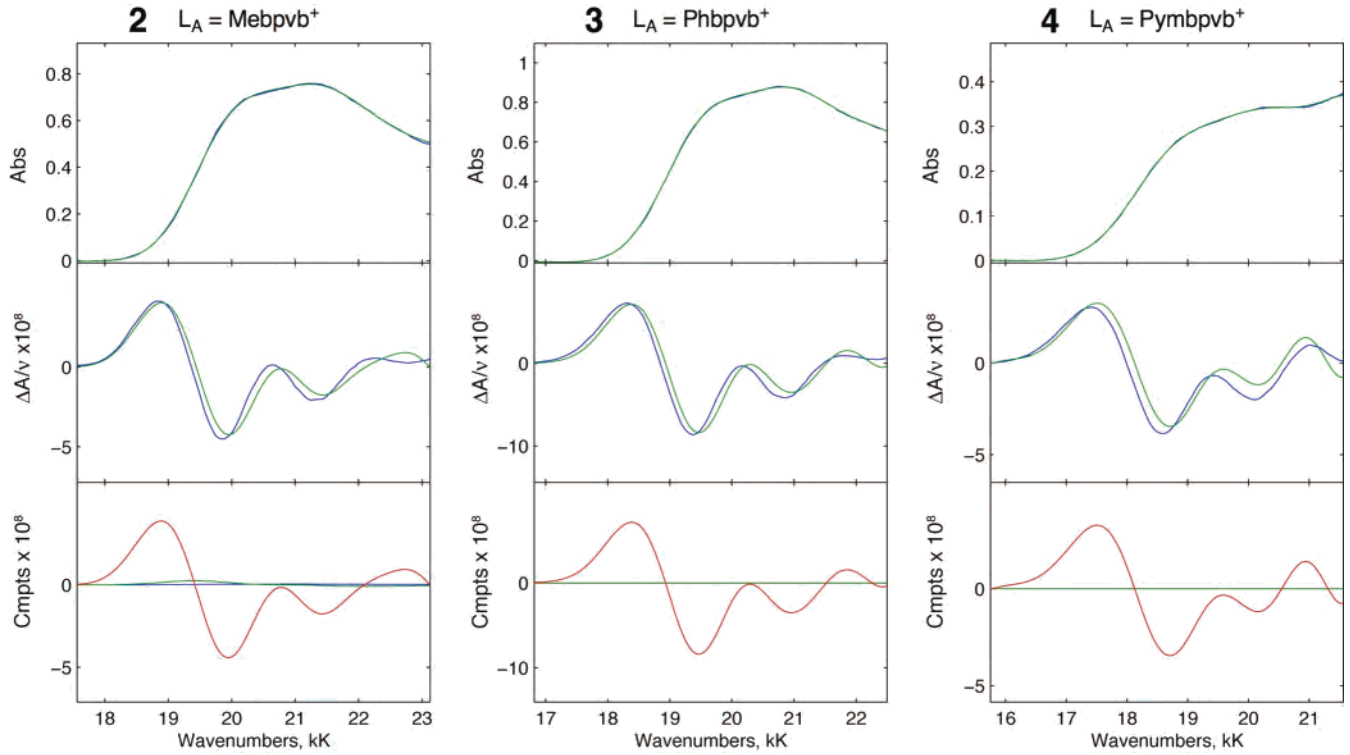

Figure 6. Absorption and electroabsorption spectra and calculated fits for the MLCT bands of salts **2**−**4** in external fields of 2.47, 2.47, and 2.48 × 10^7 V m^{-1}, respectively. Top panels, absorption spectra (blue = experimental, green = fit); middle panels, electroabsorption spectra (blue = experimental, green = fit) according to the Liptay equation;[4] bottom panels, contributions of the zeroth (blue), first (green), and second (red) derivatives of the absorption spectra to the calculated fits.

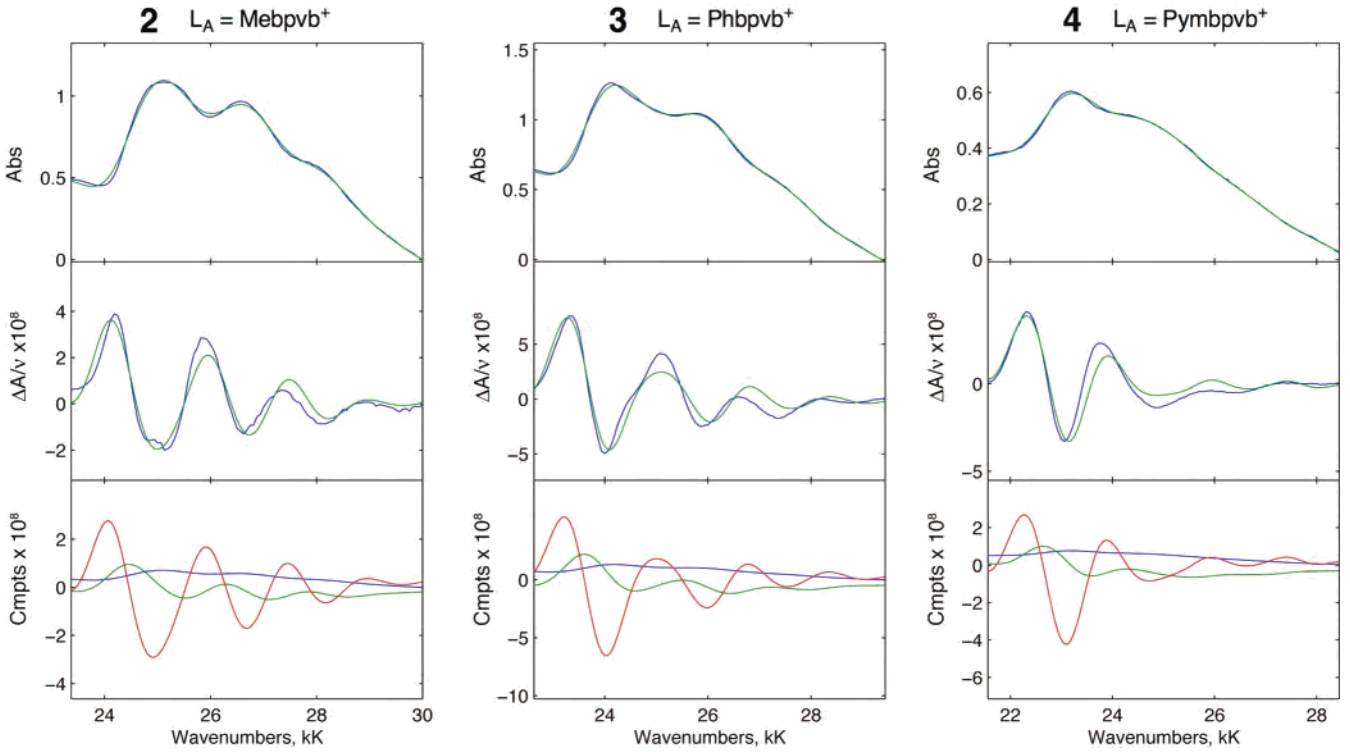

Figure 7. Absorption and electroabsorption spectra and calculated fits for the ILCT bands of salts **2**−**4** in external fields of 2.47, 2.47, and 2.48 × 10^7 V m^{-1}, respectively. Top panels, absorption spectra (blue = experimental, green = fit); middle panels, electroabsorption spectra (blue = experimental, green = fit) according to the Liptay equation;[4] bottom panels, contributions of the zeroth (blue), first (green), and second (red) derivatives of the absorption spectra to the calculated fits.

1,4-phenylene unit.[5a] Although the total β_0 response for **4** may approach that of **8**, no accompanying increase in visible transparency is achieved. Therefore, the available data indicate that the insertion of a 1,4-phenylene ring is not an especially effective strategy for combating the NLO transparency-efficiency tradeoff in these pdma complexes.

Table 7. ILCT Absorption and Stark Spectroscopic Data for Salts **2**−**4**

salt	λ_{max}[a] nm	λ_{max}[b] nm	E_{max}[b] eV	f_{os}[b]	μ_{12}[c] D	$\Delta\mu_{12}$[d] D	$\Delta\mu_{ab}$[e] D	c_b^2[f]	H_{ab}[g] cm^{-1}	β_0[h] 10^{-30} esu	β_0[tot][i] 10^{-30} esu
2	372	398	3.12	0.7	7.5	10.8	18.5	0.21	10 100	73	204
3	398	413	3.00	0.8	8.3	15.4	22.6	0.16	8900	137	340
4	416	430	2.88	0.9	9.0	21.0	27.7	0.12	7600	241	441

[a] In acetonitrile solutions at 295 K. [b] In butyronitrile glasses at 77 K. [c] Calculated from eq 2. [d] Calculated from $f_{int}\Delta\mu_{12}$ using $f_{int} = 1.33$. [e] Calculated from eq 1. [f] Calculated from eq 3. [g] Calculated from eq 4. [h] Calculated from eq 5. [i] The sum of the responses derived for the MLCT and ILCT bands.

It is perhaps worth adding a corollary at this stage. Careful inspection of the accumulated data reveals that the large increase in the MLCT-based β_0 response determined for **8** when compared with that of **2** can be traced primarily to the almost 2-fold larger value of μ_{12} for **8** (10.5 D).[23] This factor is especially significant due to the square dependence in eq 5. In contrast, in the related complexes featuring *trans*-$\{Ru^{II}(NH_3)_4(L_D)\}^{2+}$ ($L_D = NH_3$, *N*-methylimidazole or pyridine) donors, replacing the central *E*-ethenyl bond with a 1,4-phenylene unit does not greatly affect μ_{12}.[5a] Therefore, although the above conclusion concerning the transparency-efficiency tradeoff in these pdma complexes stands, it should be remembered that it is based on only limited data. It will be of interest to study further pairs of complexes of the ligands $Mebpvb^+$ and $Mebph^+$ with metal centers having similar electron donor strengths to the *trans*-$\{Ru^{II}Cl(pdma)_2)\}^+$ moiety in order to confirm whether or not the observed behavior is general.

Conclusions

Three new dipolar complex chromophores containing *trans*-$\{Ru^{II}Cl(pdma)_2\}^+$ electron donor centers connected to extended bpvb-based ligands have been prepared and fully characterized. These complexes display intense MLCT and ILCT absorptions that are relatively close in energy; both of these bands display predictable red-shifts as the electron-accepting ability of the bpvb-based ligand increases. Stark spectroscopic studies indicate that the overall quadratic NLO responses are large and increase as the ICT bands move to lower energies. Comparisons with a related polyenyl chromophore in which the central 1,4-phenylene unit of bpvb is replaced with a third *E*-ethylene bond show that a comparably large β_0 response is achieved in the present complexes only with the strongest *N*-(2-pyrimidyl)pyridinium acceptor group and with no significant gain in visible transparency. Nevertheless, the new complexes exhibit comparatively large total β_0 values, especially considering that their visible absorptions are at relatively high energy. Future studies may involve complexation of the new pro-ligands $Phbpvb^+$ and $Pymbpvb^+$ with other metal centers, although the poor solubilities of the PF_6^- salts of these species may limit their applicability and necessitate anion metathesis.

Acknowledgment. We thank the EPSRC for support in the form of a Ph.D. studentship and the provision of X-ray crystallographic facilities.

Supporting Information Available: X-ray crystallographic data in CIF format. This material is available free of charge via the Internet at http://pubs.acs.org.

IC061659U